Effect of graphene tunnel barrier on Schottky barrier height of Heusler alloy Co_2MnSi/graphene/n-Ge junction*

Gui-fang Li(李桂芳)†, Jing Hu(胡晶), Hui Lv(吕辉), Zhijun Cui(崔智军), Xiaowei Hou(候晓伟), Shibin Liu(刘诗斌), and Yongqian Du(杜永乾)

School of Electronics and Information, Northwestern Polytechnical University, Xi'an 710072, *China*

(Received 17 September 2015; revised manuscript received 16 November 2015; published online 10 January 2016)

We demonstrate that the insertion of a graphene tunnel barrier between Heusler alloy Co_2MnSi and the germanium (Ge) channel modulates the Schottky barrier height and the resistance–area product of the spin diode. We confirm that the Fermi level is depinned and a reduction in the electron Schottky barrier height (SBH) occurs following the insertion of the graphene layer between Co_2MnSi and Ge. The electron SBH is modulated in the 0.34 eV–0.61 eV range. Furthermore, the transport mechanism changes from rectifying to symmetric tunneling following the insertion. This behavior provides a pathway for highly efficient spin injection from a Heusler alloy into a Ge channel with high electron and hole mobility.

Keywords: Co_2MnSi/graphene/n–Ge junction, Fermi-level depinning, Schottky barrier height, metal-induced gap states (MIGS)

PACS: 73.40.Qv, 73.30.+y, 72.25.Dc **DOI:** 10.1088/1674-1056/25/2/027304

1. Introduction

The injection of spin-polarized electrons into semiconductor channels has attracted considerable interest recently.[1–3] To realize highly-efficient spin injection from a ferromagnetic electrode into a semiconductor channel, a highly-polarized spin injection source and a high-mobility semiconductor channel are required. The Heusler alloy Co_2MnSi is a promising candidate as a spin injection source because of its theoretically predicted half-metallicity, that is, 100% spin polarization at the Fermi energy.[4] Indeed, Jourdan *et al*. have directly observed half-metallicity in the Heusler compound Co_2MnSi in experiment.[5] Furthermore, germanium (Ge) is one of the promising semiconductor candidates because of its high bulk mobility for both electrons and holes. Thus, the combination of Co_2MnSi and a Ge channel is expected to yield highly-efficient spin injection into Ge. However, in a ferromagnetic material (FM)/Ge junction, the acceptor- and donor-like interface states in the Ge can be easily occupied by carriers penetrating the material from the FM, which can lead to the accumulation of dipole moments at the interface.[6] Thus, the Fermi level can be pinned near the charge neutrality level (CNL).[6] As the CNL of Ge is close to the valence energy band, the Schottky barrier height (SBH) of the FM/Ge junction has a weak dependence on the metal work functions and the SBH of the FM/Ge junction is relatively large, resulting in a high resistance–area (*RA*) product. The realization of an FM/Ge junction with a low *RA* product is important for various Ge-based spintronic devices.

The previous reports have suggested that the insertion of a thin insulator between an FM and the Ge is a possible method for achieving Fermi-level depinning.[7–9] Here, depinning refers to the shift of the Fermi level relative to the original strong pinning position. However, the thin-insulator defects and amorphous state could lead to an inhomogeneous interfacial structure as well as variations in the bulk film quality and thickness, all of which introduce complications to the investigation of the origin of the Fermi-level pinning.

Graphene is a potential candidate for the insulator tunneling barrier for two primary reasons: (i) it provides a highly uniform, defect-free, and thermally stable thin layer (graphene has been shown to successfully prevent interdiffusion between a ferromagnetic material and a semiconductor annealed at high temperature);[10] and (ii) it exhibits poor conductivity perpendicular to the plane, although it is very conductive in-plane.[11] Cobas *et al*. have fabricated graphene-based magnetic tunnel junctions, in which the graphene functions as a tunnel barrier, thereby demonstrating clear magnetoresistance curves at room temperature.[12] Recently, van't Erve *et al*. have reported that graphene can serve as a tunnel barrier for the spin injection from a NiFe thin film into a Si substrate using a three-terminal circuit geometry.[13] To date, however, very few studies have been published on the electrical properties of the Heusler alloy Co_2MnSi/graphene/Ge heterostructure.

In the present study, we aim to investigate the effect of the graphene tunnel barrier in a Co_2MnSi/graphene/Ge junction on the SBH. For this purpose, Co_2MnSi thin films on Ge (001) substrates with graphene layers inserted are prepared using magnetron sputtering (for Co_2MnSi thin films) and chemi-

*Project supported by the National Natural Science Foundation of China (Grant No. 61504107) and the Fundamental Research Funds for the Central Universities, China (Grant Nos. 3102014JCQ01059 and 3102015ZY043).

†Corresponding author. E-mail: gfli@nwpu.edu.cn

© 2016 Chinese Physical Society and IOP Publishing Ltd

cal vapor deposition (CVD, for graphene layers). The junctions are prepared using conventional photolithography and Ar milling, and the current versus voltage (I–V) characteristics of each junction are measured using a three-terminal circuit geometry. Subsequently, the thermionic emission model is used to quantitatively analyze the effect of the number of graphene layers on the SBH of the Co_2MnSi/graphene/Ge heterostructure.

This paper is organized as follows. Section 2 describes the experimental methods; Section 3 presents our experimental results regarding the J–V characteristics of the Co_2MnSi/graphene/Ge (001) heterostructures and an accompanying discussion; and Section 4 contains a summary of our results and conclusions.

2. Experimental method

The layer structure examined in this study was comprised of (from the substrate side) graphene/Co_2MnSi (20 nm)/Ru cap (5 nm) on a Ge (001) single-crystal substrate. The Ge substrate used here was an n-type as-doped substrate with 5-mΩ·cm resistivity. Following the removal of the native oxide using a diluted hydrofluoric acid solution, the substrate was cut into specimens with areas of 25 mm× 25 mm. The graphene was fabricated using CVD on a copper foil, and the resultant graphene/copper foil specimen was cut to sizes of 20 mm× 20 mm. The graphene surface was coated with photoresist to assist the subsequent wet-transfer process. The graphene/copper foil was immersed into ferric trichloride so that the copper was removed completely through etching, and the photoresist-coated graphene was then physically transferred onto the Ge (001) substrate. The sample was cleaned using a hydrofluoric acid solution, the photoresist was removed with acetone, and the resultant sample was finally washed using deionized water.

For samples requiring the transfer of two layers of graphene, once the first layer had been transferred, the photoresist was removed using acetone. Then the next graphene layer was transferred. Samples featuring single and double layers of graphene were examined in this study.

The prepared graphene/Ge (001) substrate was installed in a high-vacuum chamber with a base pressure of 5.0×10^{-4} Pa and a 20-nm-thick Co_2MnSi thin film was then deposited via magnetron sputtering at room temperature (RT). The sample was subsequently annealed *in-situ* at a temperature T_a of 400 °C. After growth, junctions with sizes ranging from 30 μm× 30 μm to 150 μm× 150 μm were fabricated via conventional photolithography and Ar milling. The Cr/Au was deposited directly on the Ge for ohmic contact with a specimen size of 250 μm× 250 μm. The I–V characteristics of each junction were measured using a three-terminal circuit geometry.

3. Results and discussion

Figure 1 shows the Raman spectrum of a single graphene layer, which was fabricated on the Ge (001) substrate. The typical G and 2D peaks are observed at shifts of 1596 cm^{-1} and 2685 cm^{-1}, respectively. The peak intensity ratio I_{2D}/I_G is approximately 1.62, and the relatively higher peak intensity ratio of the 2D peak compared with that of the G peak corresponds to the single-layer graphene profile. Furthermore, the full width at half maximum (FWHM) of the 2D peak is approximately 21 cm^{-1}, which is very close to 25 cm^{-1} reported for perfect single-layer graphene. Although the D peak is observed at a shift of 1352 cm^{-1}, which is related to a defect in the graphene layer, the peak intensity ratio I_D/I_G is approximately 0.06, which is appreciably small. This indicates that the prepared graphene is almost defect-free.[14]

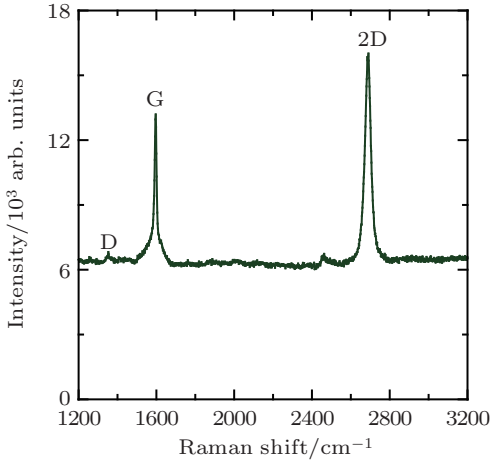


Fig. 1. Raman spectrum of single graphene layer fabricated on Ge (001) substrate.

Figure 2(a) is a schematic diagram of a layer structure consisting of a Co_2MnSi/graphene/Ge junction (labeled "2" in the figure and referred to as J2 hereafter), where the Cr/Au thin films were grown directly on the Ge substrate for ohmic contact with junctions 1 and 3. The I–V characteristics of J2 were measured using the three-terminal circuit geometry. A bias voltage V was applied between terminals 1 and 2, a current meter was used to measure the current across J2, and the V across J2 was obtained through measurement of the V between terminals 2 and 3. For a negative (positive) bias, the Co_2MnSi/graphene/Ge junction was reverse (forward) biased.

Figure 2(b) shows the typical J–V characteristics of the Co_2MnSi/graphene/Ge (001) heterostructures with different numbers of graphene layers at RT. Following the insertion of a single graphene layer ($t = 1$), the reverse-biased current increases in comparison to the Co_2MnSi/Ge Schottky diode ($t = 0$), indicating that the Fermi level is depinned. However, when two graphene layers are used ($t = 2$), the reverse- and forward-biased currents decrease. Most importantly, the J–V characteristics are near symmetric with respect to the bias

polarity, and the transport mechanism changes from rectifying (for Co_2MnSi grown directly on the Ge (001) substrate) to symmetric tunneling following the insertion of two graphene layers. Moreover, the *RA* products of the contacts at a reversed bias of −0.20 V are 0.78 Ω·cm^2, 0.19 Ω·cm^2, and 1.2 Ω·cm^2 for $t = 0$, 1, and 2, respectively.

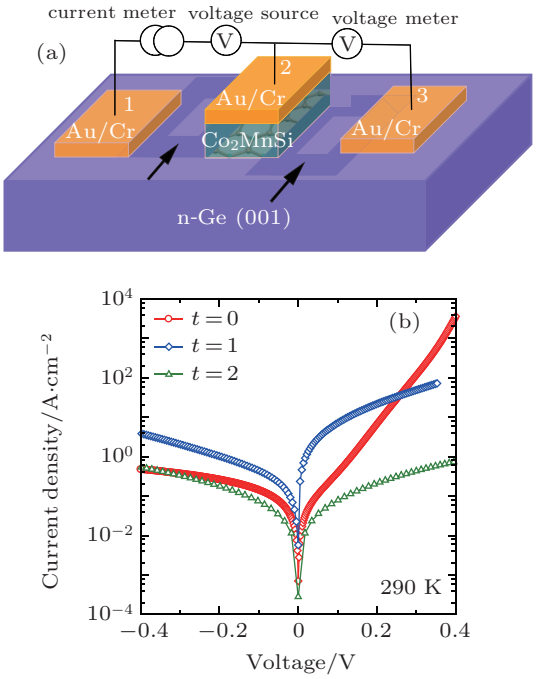


Fig. 2. (color online) (a) Schematic diagram of device structure and three-terminal circuit geometry for measurement of *I*–*V* characteristics. (b) Typical *J*–*V* characteristics of Co_2MnSi/graphene/Ge (001) heterostructures with different numbers of graphene layers at RT.

For a quantitative analysis of the effect of the graphene layer insertion on the SBH of the Co_2MnSi/graphene/Ge junction, the thermionic emission model is adopted.[15] This model is expressed as

$$J = A^* T^2 \exp\left(-\frac{q\phi_b}{kT}\right) \exp\left(\frac{qV}{nkT}\right)\left[1 - \exp\left(-\frac{qV}{kT}\right)\right], \tag{1}$$

where A^* is the Richardson constant, T is the temperature, q is the electron charge, k is the Boltzmann constant, ϕ_b is the effective SBH, n is an ideality factor, and V is the applied bias voltage.

For $V \gg kT/q, 1 - \exp(-qV/kT) \approx 1$ ($kT/q = 18$ eV–26 mV for T ranging from 210 K to 300 K). Thus, equation (1) can be expressed as

$$\ln\left(\frac{J}{T^2}\right) = -\frac{q}{k}\left(\phi_b - \frac{V}{n}\right)\frac{1}{T} + \ln A^*. \tag{2}$$

For a plot of $\ln(J/T^2)$ versus $1/T$, also called the Richardson plot, a linear line is found with a slope of $a = -(q/k)(\phi_b - V/n)$. In this study, a set of a values were obtained for different V. Then, plotting a as a function of V, a linear curve with slope $-(q/k)(1/n)$ was obtained along with a y-axis intercept of ϕ_b.

Figure 3(a) shows the Richardson plots of the Co_2MnSi/single-graphene ($t = 1$)/Ge (001) junction for $V = 0.15$ V–0.25 V. The a is extracted from the linear fitting of each plot and then plotted as a function of V in Fig. 3(b). From the linear fitting of the latter plot, n and ϕ_b are found to be 1.45 and 0.39 eV, respectively. Note that $\ln A^*$ is not considered in the calculation of the SBH for the Co_2MnSi/graphene/Ge (001) junction; this is because the additional contribution from the tunneling probability through the graphene could be viewed as a modification of the conventional A^*.[16]

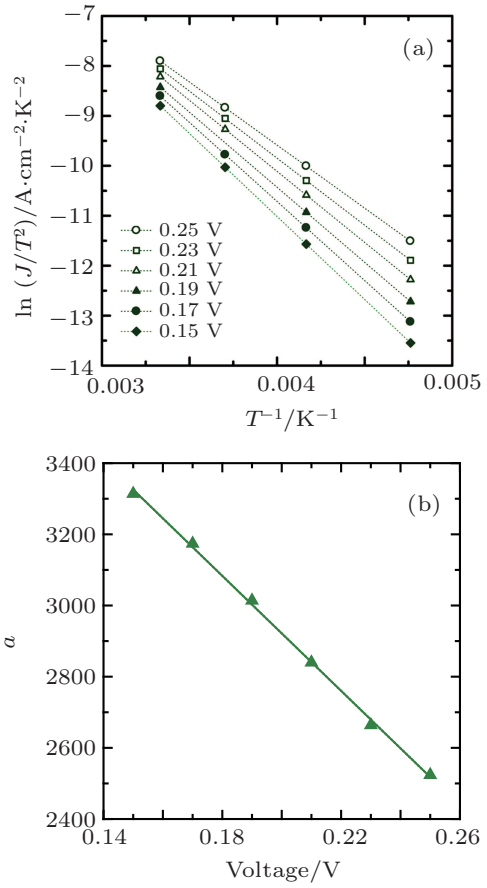


Fig. 3. (color online) (a) Richardson plots of Co_2MnSi/single-graphene ($t = 1$)/Ge (001) junction for $V = 0.15$ V–0.25 V. (b) Plot of $a = -(q/k)(\phi_b - V/n)$ versus V for Co_2MnSi/single-graphene ($t = 1$)/Ge (001) junction.

Table 1. The Schottky barrier height and ideality factor (n) of Co_2MnSi/graphene/Ge (001) junctions with different graphene tunnel barrier thicknesses.

The number of single-layer graphene	Schottky barrier height/eV	Ideality factor n
0	0.61	1.12
1	0.39	1.45
2	0.34	2.41

The SBH and n values of the Co_2MnSi/graphene/Ge (001) junctions with different numbers of graphene layers are extracted and listed in Table 1. For the Co_2MnSi grown directly on the Ge (001) substrate, n is slightly larger than expected

at 1.0. This may be due to the high doping concentration of the n-Ge substrate. The n increases with increasing t, which is consistent with a change in the dominant transport mechanism from thermionic emission ($n \approx 1$) to an additional tunneling process ($n > 1$).[16] Moreover, the SBH exhibits a negative dependence on t, which is consistent with the metal-induced gap states (MIGS) model.[17,18] Very little interface modulation of the Schottky junction behavior was observed for the Co_2MnSi/single graphene/Ge junction.

It is well known that MIGS are formed by tailing of the wave function into the semiconductor band-gap. Therefore, it is very likely that tailing suppression due to the presence of the ultrathin graphene layer caused the change in the SBH. However, when two layers of graphene were inserted between Co_2MnSi and the Ge channel, the tunneling dominated the transport mechanism. Thus, this result provides an evidence that the MIGS are the most plausible mechanism for the strong Fermi-level pinning at the Co_2MnSi/Ge interface. As the graphene-layer thickness increases, the SBHs decrease significantly and the I–V characteristics become almost symmetric with respect to the bias polarity for the Co_2MnSi/double-graphene ($t = 2$)/Ge junction, which is promising as regard to the realization of spin injection and detection from highly spin-polarized Co_2MnSi thin films to Ge channels featuring high electron and hole mobility.

4. Conclusion

The effect of the inserted graphene layer on the Schottky barrier height of a Co_2MnSi/graphene/Ge junction was investigated with one or two graphene layers. It was found that the Fermi level was depinned and the SBH was significantly decreased (from 0.61 eV to 0.34 eV) following the insertion of a graphene layer. Furthermore, the measured SBH depended on the number of graphene layers, which is consistent with the metal-induced gap states model. Our results demonstrate that graphene insertion can be useful for the realization of spin injection and detection from highly spin-polarized Co_2MnSi thin films to Ge channels featuring high electron and hole mobility.

References

[1] Lou X, Adelmann C, Crooker S A, Garlid E S, Zhang J, Madhukar Reddy K S, Flexner S D, Palmstrøm C J and Crowell P A 2007 *Nat. Phys.* **3** 197

[2] Dash S P, Sharma S, Patel R S, Jong de M P and Jansen R 2009 *Nature* **462** 491

[3] Zhou Y, Han W, Chang L T, Xiu F, Wang M, Oehme M, Fischer I A, Schulze J, Kawakami R K and Wang K L 2011 *Phys. Rev. B* **84** 125323

[4] Picozzi S, Continenza A and Freeman A J 2002 *Phys. Rev. B* **66** 094421

[5] Jourdan M, Minár J, Braun J, Kronenberg A, Chadov S, Balke B, Gloskovskii A, Kolbe M, Elmers H J, Schönhense G, Ebert H, Felser C and Kläui M 2014 *Nat. Commun.* **5** 3974

[6] Nishimura T, Kita K and Toriumi A 2007 *Appl. Phys. Lett.* **91** 123123

[7] Schmidt G, Ferrand D, Molenkamp L W, Filip A T and van Wees B J 2000 *Phys. Rev. B* **62** R4790

[8] Rashba E I 2000 *Phys. Rev. B* **62** R16267

[9] Fert A and Jaffres H 2001 *Phys. Rev. B* **64** 184420

[10] Li G, Liu S, Yang S and Du Y 2015 *J. Nanomater.* **2015** 575401

[11] Krishnan K S and Ganguli N 1939 *Nature* **144** 667

[12] Cobas E, Friedman A L, van't Erve O M J, Robinson J T and Jonker B T 2012 *Nano Lett.* **12** 3000

[13] van't Erve O M J, Friedman A L, Cobas E, Li C H, Robinson J T and Jonker B T 2012 *Nat. Nanotechnol.* **7** 737

[14] Wang G, Zhang M, Zhu Y, Ding G, Jiang D, Guo Q, Liu S, Xie X, Chu, P K, Di Z and Wang X 2013 *Sci. Rep.* **3** 2465

[15] Mönch W 2004 *Electronic Properties of Semiconductor Interface* (Berlin: Springer)

[16] Sze S M and Ng K K 2007 *Physics of Semiconductor Devices*, 3rd edn. (New Jersey: Willey)

[17] Teroff J 1984 *Phys. Rev. Lett.* **52** 465

[18] Louie S G and Cohen M L 1976 *Phys. Rev. B* **13** 2461